

Degradation of aged nitrocellulose investigated by thermal analysis and chemiluminescence

Jozef Rychlý · Agnes Lattuati-Derieux ·
Lyda Matisová-Rychlá · Katarína Csomorová ·
Ivica Janigová · Bertrand Lavédrine

Received: 11 March 2011 / Accepted: 15 June 2011 / Published online: 30 June 2011
© Akadémiai Kiadó, Budapest, Hungary 2011

Abstract Non-isothermal thermogravimetry, differential scanning calorimetry and chemiluminescence were used for characterization of degradation of pre-aged nitrocellulose in order to elucidate the optimal route of extrapolation of rate constants from the region of the autoaccelerated reaction to lower temperatures. First order rate constants, the one characterizing the decomposition of nitrocellulose in the rate auto-accelerating region and the two constants corresponding to the slow process in induction period of nitrocellulose decomposition were shown to provide a sufficient description. The rate constants determined for several temperatures were shown to depend on the amount of char residue which is formed from pre-aged samples after the thermogravimetry runs from 40 to 550 °C.

Keywords Nitrocellulose · Ageing of · Thermogravimetry · Differential scanning calorimetry · Chemiluminescence · Rate constants

Introduction

Nitrocellulose is a derivative of natural cellulose obtained by nitration. It has many interesting properties and applications. Nitration of cellulose is an essential pre-requisite

for production of microporous membranes that show properties of excellent blotting agents. Cellulose nitrate films became popular in the late 1880s because of their physical properties which made them ideal for photography. Into the early 1950s, cellulose nitrate films were used mostly for still photography, but they were also used for X-ray films and motion picture films. Cellulose nitrate became also very popular as the material for different technological and medical products including hair combs, toys, casings and imitations for ivory, tortoiseshells and may be found in many historical artifacts collections [1]. After 1950, the production of cellulose nitrate films was stopped and it was replaced by less dangerous cellulose acetate or similar materials. The reason was that museums and photographic archives were often jeopardized by a very serious fire risk as nitrocellulose burns quickly with an intense flame. The rate of combustion for cellulose nitrate film is about 15 times faster than that of wood. Fully nitrated cellulose has nitrogen content 14.2%, for nitrocellulose coatings and printing inks nitrogen content is between 10.7 and 12.3%. Above this value of nitrogen, nitrocellulose can perform the explosive properties [2, 3].

Various data not always uniform are available on the thermal behavior and kinetics of decomposition of nitrocellulose compounds [4–11]. When one attempts to compare the rate constants for a given temperature and/or activation energies, the enormously large scatter of data may be found in the literature. This may be due to following reasons.

- (1) According to the thermogravimetry and DTA data [10] it was verified that in dependence on nitrate content (from 12.5 to 13.9% of nitrogen) the decomposition of nitrocellulose started at about 192 °C and this temperature increased with decreasing nitrogen

J. Rychlý (✉) · L. Matisová-Rychlá · K. Csomorová ·
I. Janigová
Polymer Institute, Slovak Academy of Sciences, Dúbravská
cesta 11, 84541 Bratislava, Slovakia
e-mail: upoljory@savba.sk

A. Lattuati-Derieux · B. Lavédrine
Centre de Recherche sur la Conservation des Collections,
Muséum National d'Histoire Naturelle, MCC, CNRS,
36 rue Geoffroy-Saint-Hilaire, 75005 Paris, France

content. In that temperature region, auto-accelerated decomposition of nitrocellulose occurs. Extrapolation of data from the temperature region of auto-accelerating reaction to lower temperature region represents a problem. DSC and TG measurements usually cover relatively narrow temperature interval where some declinations may be observed and for the interval of low temperature these methods are not sensitive enough.

- (2) A lot of non-isothermal models applied which are sometimes used without further discrimination.

The inherent and irreversible degradation of nitrocellulose brings also the problems to conservators where attention is focused on degradation of nitrocellulose in lacquers and furniture coatings [12, 13].

In this article, nitrocellulose membranes before and after ageing at 130 °C in air were investigated by means of non-isothermal differential scanning calorimetry (DSC), thermogravimetry (TG), and chemiluminescence (CL). This temperature enabled to evaluate the interpretation of slow degradation reaction at lower temperatures and accelerated decomposition occurring at higher temperatures with an attempt to link both temperature regions into one model. No effect of ageing on nitrocellulose at 50 °C lasting until 6 weeks that was analysed by thermogravimetry has been found on activation energy of its decomposition [3].

While DSC and thermogravimetry were largely used for assessment of the progress of nitrocellulose degradation and also for the evaluation of stability of other energetic materials, it was of interest to compare the results of both methods with those from non-isothermal chemiluminescence method focused on the study of the transformations of solid residue remaining during degradation. Chemiluminescence technique was until now used only for measurements of NO and NO₂ gases from 20 to 150 °C released from degrading nitrocellulose in air [14] and two sets of the rate constants were determined for temperatures below 80 °C and above 100 °C.

For observation of chemiluminescence from polymers, oxygen must be present at the onset of heating, or throughout the entire process of polymer degradation [15–22]. In nitrogen, the emission of the light is considerably lower reflecting the energetic gain from recombination of alkyl or alkoxy radicals and from the consumption of oxygen residuals present in the sample. The necessary prerequisite of the chemiluminescence observation is the parallel formation of energy acceptor like carbonyl groups or oxygen capable of transformation of the chemical energy into the light. The essential polymer degradation reactions that exhibit chemiluminescence include: (1) hydroperoxides decompositions initiating oxidation and degradation; and (2) direct scission of the main polymer

chains producing alkyl and in the presence of oxygen peroxy radicals. In the case of nitrocellulose, there may be also formed excited nitrogen oxides [14].

As for non-isothermal chemiluminescence from polymers, it was Wendlandt who first published a number of important papers [23–27]. The output of the chemiluminescence method is thus specifically related to free radical processes occurring in the material and the effect of oxygen on the rate of nitrocellulose degradation may well be assessed.

Experimental

Thermogravimetry (TG)

Thermogravimetry experiments were performed using a Mettler-Toledo TGA/SDTA 851° instrument with a nitrogen or oxygen atmosphere (30 mL min⁻¹). Samples were heated from room temperature to 550 °C using the rate 10 °C min⁻¹. Indium and aluminum were used for temperature calibration. The experimental runs were corrected on the buoyancy effect.

Chemiluminescence (CL)

Chemiluminescence measurements were carried out on the luminometer Lumipol 3 produced at the Polymer Institute of SAS, Bratislava. The intensity of the emitted light (in counts/s) was recorded under non-isothermal conditions as curves of intensity versus temperature. Heating rate was 5 °C min⁻¹. The instrument dark count rate was 2–3 counts⁻¹. Samples of ~1 mg were weighed onto aluminum pans with a diameter of 9 mm and put into the oven of the CL apparatus. The oxygen and nitrogen flow rate above the sample was 50 mL min⁻¹.

Differential scanning calorimetry (DSC)

DSC measurements were performed using a Mettler-Toledo DSC 821° differential scanning calorimeter, in nitrogen and oxygen atmospheres with flow rates of 50 mL min⁻¹. Indium was used for calibrating the temperature and the heat of fusion. Samples were heated from room temperature to 550 °C with heating rates 5 and 10 °C min⁻¹.

Samples

Nitrocellulose sample was a white membrane used in biology; it is produced by GE Healthcare (US). The quantitative elemental analysis indicated weight percents of carbon, hydrogen and nitrogen 27.20, 2.93, and 11.76%,

respectively. Nitrocellulose contains two nitro groups per one glucopyranosyl unit of the cellulose. The samples were aged for periods varying from 6 h to 16 days at 130 °C in open conditions of ambient air and uncontrolled relative humidity. The aged samples were collected at intervals 6 h, 1, 2, 4, 8, and 16 days, respectively. Visual observations confirmed the increase of the yellowing with time of ageing already after 2 days of ageing. The samples became slightly brown after 4 days of ageing and dark brown when aged longer. During ageing samples became brittle. The formation of acid volatiles was evaluated by pH measurements of aqueous extract (1.5 mg of sample was immersed in 150 µl of pure water with a stirring bar, during 3 h). This extract became significantly acidic with the duration of ageing. pH changed from 6.5 (for the reference sample) to 2.5 (for 16 days-aged sample). The pH values obtained after 1, 2, 4, and 8 days were 4.8, 4.7, 3.5, and 3.0, respectively. This acidity is obviously due to the nitric acid which is formed during nitrocellulose degradation.

The ATR spectrum of a reference sample of original nitrocellulose membrane is given on the Fig. 1.

Mathematical modelling of experimental results obtained by non-isothermal thermogravimetry

The formation of volatile degradation products as observed by non-isothermal thermogravimetry represents an integral process. The complex non-isothermal thermogravimetry curve obtained is apparently composed of several independent processes. In our methodology, each process was described by the first-order scheme of the mass *m* loss, i.e., $-\frac{dm}{dt} = km$. In a non-isothermal mode, $-\frac{dm}{m} \frac{dT}{dt} = A \exp\left(-\frac{E}{RT}\right)$, where $\beta = \frac{dT}{dt}$ is a linear heating rate, and *k* is a corresponding rate constant expressed in the Arrhenius' form. *A*, *E*, and *T* denote pre-exponential factor, activation

energy, and absolute temperature, respectively. After integration, we obtain

$$m = m_0 \exp \left[-\frac{A}{\beta} \int_{T_0}^T \exp\left(-\frac{E}{RT}\right) dT \right],$$

i.e., the function of the mass *m* decaying with an increasing temperature. For the process composed of *j* temperature-dependent components—"waves", we have

$$m = m_0 \sum_{i=1}^j \alpha_i \exp \left[-\frac{A_i}{\beta} \int_{T_0}^T \exp\left(-\frac{E_i}{RT}\right) dT \right]. \tag{1}$$

Here α_i is the contribution of the respective process composing the initial mass *m*₀.

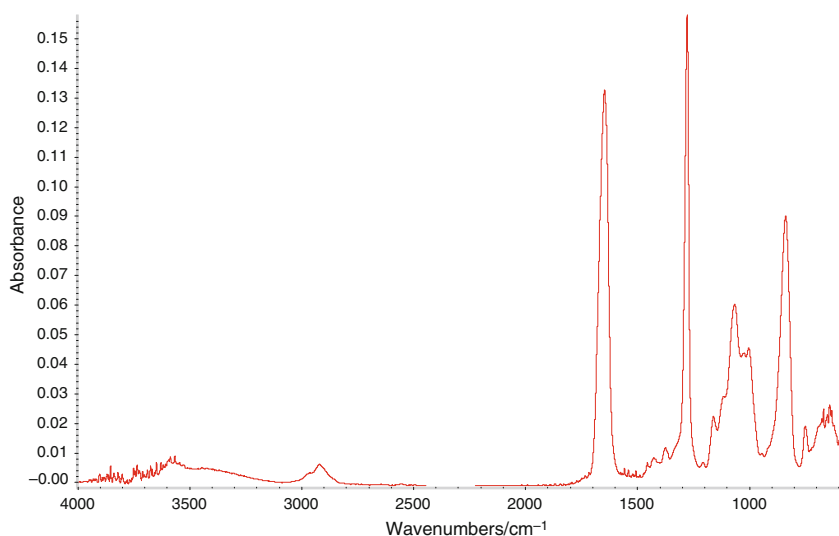
Provided that mass changes are expressed as a percentage of the original mass *m*₀, parameters *a*_{*i*}, *A*_{*i*}, *E*_{*i*} may be found by a program of the nonlinear regression analysis applied to curves of the experimental mass *m* versus temperature *T*, from the initial temperature *T*₀ to a final temperature *T* of the experiment. The rate constant, *k*_{*i*}, corresponding to a given temperature is expressed as

$$k_i = A_i \exp(-E_i/RT)$$

Non-isothermal DSC and chemiluminescence methods

While non-isothermal thermogravimetry enables to cover the decomposition of nitrocellulose from the mass loss and extends into the temperature interval of transformation of char residue, DSC covers relatively narrow temperature interval of the exothermic process occurring very fast in an explosion like manner. The disadvantage of DSC experiments is very difficult determination of the base line over a large temperature interval which should be subtracted from the experimental curve when evaluating the respective rate

Fig. 1 ATR spectrum (OMN) of nitrocellulose membrane (reference sample 0)



parameters. On the other hand the chemiluminescence method yields a very stable base line which under non-isothermal conditions changes only slightly and may be easily subtracted from the experimental curve. Chemiluminescence intensity appears to be proportional to the rate of the degradation process that may be thus assessed even from ambient conditions. In this article, the estimation of kinetic experiments based on DSC and chemiluminescence takes into account the actual intensity of the signal (DSC and I) which is divided by the remaining surface below the curve and for the first order of decomposition reaction it should be proportional to the remaining concentration of non-decomposed nitrocellulose. For the first-order rate constant, we thus have:

$$\frac{k}{\beta} = \frac{\int_{T_{\text{init}}}^{\infty} \text{DSC} dT}{\int_{T_{\text{init}}}^{\infty} \text{DSC} dT - \int_T^{\infty} \text{DSC} dT} = \frac{\int_{T_{\text{init}}}^{\infty} I dT}{\int_{T_{\text{init}}}^{\infty} I dT - \int_T^{\infty} I dT} \quad (2)$$

Here β is the linear rate of heating, DSC and I are signals of DSC and chemiluminescence for the respective temperature and $\int_{T_{\text{init}}}^{\infty} \text{DSC} dT$ and $\int_{T_{\text{init}}}^{\infty} I dT$ are the total surfaces below DSC and chemiluminescence curve from the initial temperature T_{init} to the end of the line while $\int_T^{\infty} \text{DSC} dT$ and $\int_T^{\infty} I dT$ are the surfaces from the temperature T to the end of the line.

Results and discussion

From the Fig. 2, it may be seen how nitration destabilizes the original cellulose. The effect of oxygen on the degradation of nitrocellulose is not almost visible on TG experimental runs, while that for pure cellulose it is significant. This may be explained by the intervention of oxygen into the initiation reaction of oxidation via the carbon atom 6 of glucopyranosyl unit of the cellulose, while in the case of nitrocellulose, the initiation occurs independently via the scission of bonds $-\text{O}-\text{NO}_2$. Oxygen affects the oxidation in the subsequent stages of the reaction. The loss of volatiles is also much sharper for nitrocellulose than for cellulose. At high temperatures there remains a certain amount of char residue which under nitrogen loses the weight slowly. In oxygen, an acceleration of the char residue oxidation may be observed above 420 °C (Fig. 2).

Non-isothermal thermogravimetry runs of the set of nitrocellulose samples in nitrogen at the rate of heating $10 \text{ }^\circ\text{C min}^{-1}$ are seen in the Fig. 3. It is worth of noticing that with the progress of the sample ageing at $130 \text{ }^\circ\text{C}$ in air

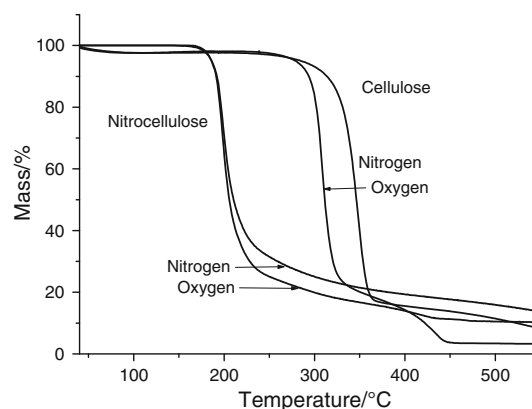


Fig. 2 Comparison of nonisothermal thermogravimetry runs of cellulose and nitrocellulose in nitrogen and oxygen. The rate of heating $10 \text{ }^\circ\text{C min}^{-1}$

the temperature of the inflexion point shifts to higher values (Fig. 3) being $197.7 \text{ }^\circ\text{C}$ for reference sample and $207.7 \text{ }^\circ\text{C}$ for the most aged sample. This corresponds with the gradual loss of nitro groups from nitrocellulose due to ageing. At the same time, the percentage of the char residue which remains after thermogravimetry experiment at $550 \text{ }^\circ\text{C}$ slowly increases.

The set of parameters obtained from non-isothermal thermogravimetry experiments (Eq. 1) such as the activation energy and fractional values α of respective components released as volatiles or remaining as a char residue is given in the Table 1. Activation energy estimated according to Eq. 1 for release of volatiles decreases with the progress of nitrocellulose ageing being 260 kJ mol^{-1} for the reference and 130 kJ mol^{-1} for the sample aged 16 days in air at $130 \text{ }^\circ\text{C}$. At the same time, the rate constants k_1 calculated from Arrhenius parameters for $130 \text{ }^\circ\text{C}$ increase, while those for $200 \text{ }^\circ\text{C}$ decrease with the extent of nitrocellulose ageing. Figure 4 shows on the quality of the

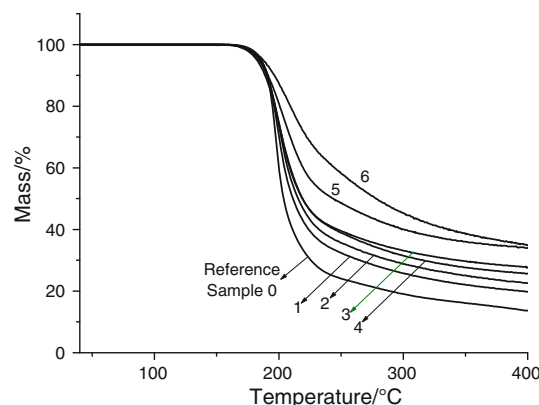


Fig. 3 Nonisothermal thermogravimetry of aged nitrocellulose samples, nitrogen, the rate of heating $10 \text{ }^\circ\text{C min}^{-1}$

fit of several selected lines when using the theoretical parameters from the Table 1.

The rate constants of the first order determined from the parameters of the fit using Eq. 1 for 130 and 200 °C correlate with the percentage of the char residue determined from non-isothermal TG runs; those at 130 °C with an increasing percentage of the char residue increase (Fig. 5). Although the extrapolation of rate constant to 130 °C from non-isothermal TG is affected by the faster auto-accelerating decomposition process occurring above 190 °C, the increasing tendency of the rate constants indicate that there may occur the effect of the forming char on the autocatalysis of decomposition of nitrocellulose. Until now the autocatalysis in decomposition of nitrocellulose was ascribed to the effect of nitric acid. From the flammability experiments on some energetic materials, we know that the glowing char may act as a spark of the ignition of the explosive course.

With the extent of nitrocellulose ageing there occurs also the shift of the maximum of DSC exotherm to higher temperatures, while the peak height is reduced (Fig. 6). The essential data from DSC measurements in nitrogen for the rates of heating 5 and 10 °C min⁻¹ are summarized in the Table 2 indicating quite a good repeatability of respective experiments. As expected, the maximum of the exotherm is shifted to higher temperatures for the higher rate of heating.

Provided that the surface below DSC exotherm is proportional to the concentration of unreacted nitro groups and the kinetics of nitrocellulose decay in membrane during its ageing at 130 °C is approximated by the first-order scheme (Fig. 7), we see that the rate constant of nitrocellulose degradation is somewhat lower than that found by extrapolation from chemiluminescence measurement. However, the difference is not as large (Table 3).

Regardless of the observation done by thermogravimetry namely that the effect of oxygen on nitrocellulose degradation is not as distinct as it is in the case of cellulose,

Table 1 The kinetic parameters determined from non-isothermal thermogravimetry records in nitrogen for aged nitrocellulose, the rate of heating 10 °C min⁻¹, α_1 is the fraction of volatiles found from Eq. 1, A_1 , E_1 is the pre-exponential factor and activation energy

Sample	Aged at 130 °C in air, days	α_1	α_2	α_3	A_1/s^{-1}	$E_1/kJ\ mol^{-1}$	k_1/s^{-1} 130 °C	k_1/s^{-1} 200 °C
Reference	0	0.622	0.171	0.212	7.3e26	259.9	2.6e-7	2.3e-2
0								
1	0.25 (6 h)	0.539	0.192	0.274	1.6e22	218.5	1.2e-6	1.7e-2
2	1	0.522	0.185	0.297	3.1e18	185.9	3.7e-6	1.3e-2
3	2	0.500	0.172	0.332	3.3e17	177.2	5.2e-6	1.2e-2
4	4	0.506	0.188	0.309	3.1e15	159.1	1.0e-5	1.1e-2
5	8	0.415	0.200	0.388	5.8e13	144.5	1.5e-5	8.3e-3
6	16	0.299	0.295	0.408	8.9e11	129.5	1.9e-5	5.5e-3

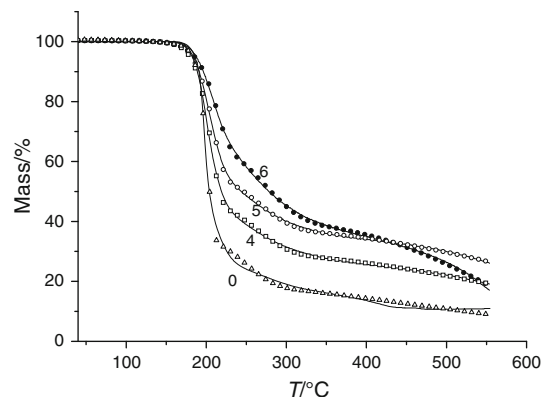


Fig. 4 The theoretical fit of thermogravimetry course of some aged nitrocellulose samples by the Eq. 1. Points denote the fitted data

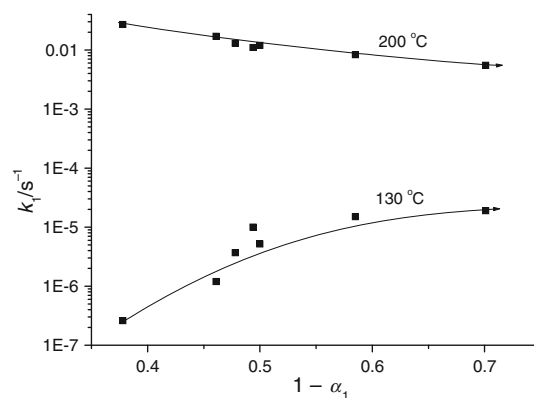


Fig. 5 The correlation of the rate constants approximated from the set of experiments (Fig. 2; Table 1) with a char residue $1 - \alpha_1$

it still exists. In the Fig. 8, we may see the comparison of DSC exotherms for the rate of heating 5 °C min⁻¹; the surface below DSC exotherm in nitrogen is 66% of that for oxygen.

When comparing DSC and chemiluminescence records in oxygen, we see another peak appearing in the latter case (Fig. 9) which is likely to correspond with the oxidation of

formation of volatiles from nitrocellulose, and k_1 is the rate constant of nitrocellulose degradation into volatiles (α_2 and α_3 are fractions attributed to the transformation of char residue)

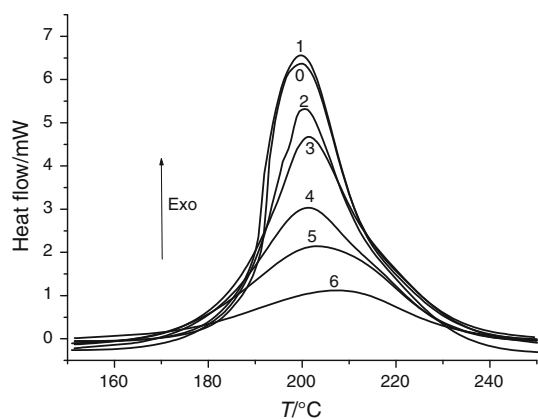


Fig. 6 DSC runs in nitrogen of aged samples of nitrocellulose

char residue. This is confirmed by the gradual development of this peak when examining more aged samples (Fig. 10). With longer time of nitrocellulose ageing, this latter peak starts to predominate, and it is shifted to lower temperatures. In nitrogen experiments, this peak was not observed (Fig. 11). We may also see that in the presence of nitrogen the chemiluminescence signal that is lower than that in oxygen, is also important.

Figure 12 shows how chemiluminescence intensity changes with the stepwise increase of temperature. The experiment was performed so that temperature was kept constant for a certain time and the chemiluminescence run in oxygen occurred isothermally. The fast increase of chemiluminescence intensity took place already at 180 °C. At lower temperatures, the isothermal parts of the decomposition curve gave the stationary levels of the intensity of light emission eventually being accompanied by the slow decay.

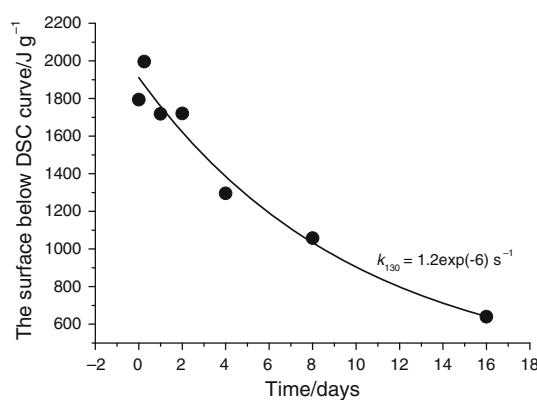


Fig. 7 Decay of the surface below DSC exotherm for ageing of nitrocellulose in air at 130 °C

Figure 13 demonstrates the different temperature regions of nitrocellulose decomposition in both nitrogen and oxygen. While at temperatures below 190 °C, the activation energy is 89 kJ/mole and extrapolation of the rate constant to lower temperature seems to be quite reliable, at 194 °C there occurs a sharp increase of activation energy to a very high value (>500 kJ/mole) which is typical for the explosion like course of decomposition. One has to admit that any extrapolation from the temperature interval of the explosion-like course has no sense because extremely low rate constants for the decomposition of NC are obtained at, e.g., ambient conditions. The chemiluminescence experiment appears to show on linkage between slow decomposition of nitrocellulose and explosion like course.

The temperature interval well below 190 °C which corresponds to the activation energy 89 kJ mol⁻¹ gives evidently “good” rate constants when extrapolating to lower temperatures (Table 3). This allows to predict the

Table 2 DSC parameters for the aged nitrocellulose—comparison of parallel experiments in nitrogen at the rate of heating 5 and 10 °C min⁻¹

Sample	Surface below the exotherm/J g ⁻¹		Peak height/Wg ⁻¹		Temperature of the peak/°C	
	5 °C min ⁻¹	10 °C min ⁻¹	5 °C min ⁻¹	10 °C min ⁻¹	5 °C min ⁻¹	10 °C min ⁻¹
Reference	1870	1723	6.65	11.35	200.07	207.8
0	1718	1969	6.17	12.05	199.96	208.8
1	2029	1858	6.82	12.24	199.93	207.45
	1964	1811	6.55	11.54	199.46	207.10
2	1719	1845	5.62	10.9	200.57	206.5
3	1746	1895	5.02	9.26	201.03	207.5
	1696	–	4.70	–	201.95	–
4	1319	1673	3.13	8.00	201.22	207.6
	1274	1489	3.30	7.51	201.18	207.7
5	1144	1292	2.39	4.41	203.2	210.8
	972	1401	2.13	4.61	202.52	210.8
6	521.90	779	1.08	2.2	207.84	218.9
	759.40	653	1.32	2.2	206.82	215.5

Table 3 The rate constants of the first order of nitrocellulose decomposition—an overview

k/s^{-1} 50 °C	k/s^{-1} 130 °C	k/s^{-1} 200 °C	Note
1.3e-15	2.6e-7	0.0229	This article, reference sample 0 TG in nitrogen
1.3e-13	1.2e-6	1.7e-2	This article, sample 1 TG in nitrogen
4.3e-12	3.7e-6	1.3e-2	This article, sample 2 TG in nitrogen
1.1e-11	5.2e-6	1.2e-2	This article, sample 3 TG in nitrogen
8.7e-11	1.0e-5	1.1e-2	This article, sample 4 TG in nitrogen
3.6e-10	1.5e-5	8.3e-3	This article, sample 5 TG in nitrogen
1.0e-9	1.9e-5	5.5e-3	This article, sample 6 TG in nitrogen
–	5.0e-9	0.0095	This article, reference sample DSC in nitrogen
2.0e-9	4.5e-6	0.0032	This article, reference sample, CL in nitrogen
4.2e-8	3.1e-6	–	This article, NC aged 6 h at 130 °C in air CL in oxygen
–	1.2 e-6	–	This article DSC surface of aged samples, 130 °C, air
1.6e-11	6.0e-6	0.0083	Paper [5]—autocatalytic model
1.2e-10 (below 80 °C)	2.9e-6 (above 100 °C)	7.8e-3	Paper [14] Air, NO _x release
5.0e-9	4.8e-4	0.493	ASTM method, paper [10], Helium, DSC
7.0e-9	5.7e-4	0.489	Method by Ozawa, paper [10], Helium, DSC

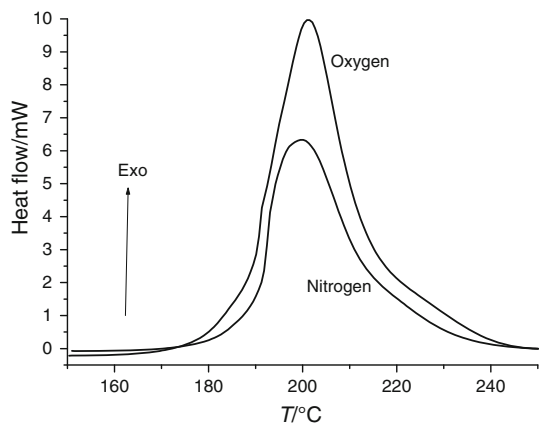


Fig. 8 Comparison of DSC runs for nitrocellulose (reference sample 0) in oxygen and in nitrogen. The rate of heating 5 °C min⁻¹

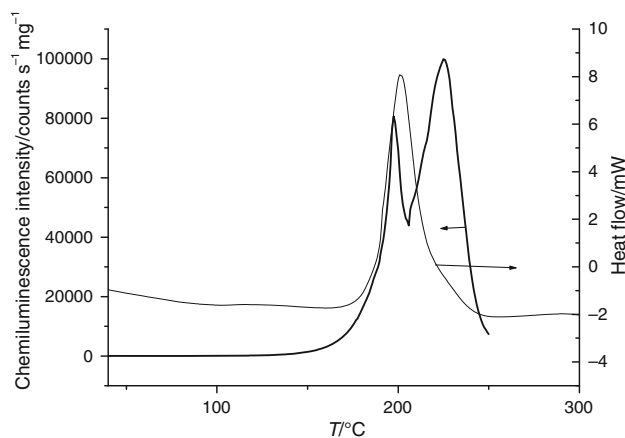


Fig. 9 Comparison of nonisothermal chemiluminescence and DSC runs in oxygen for nitrocellulose, sample 0, the rate of heating 5 °C min⁻¹

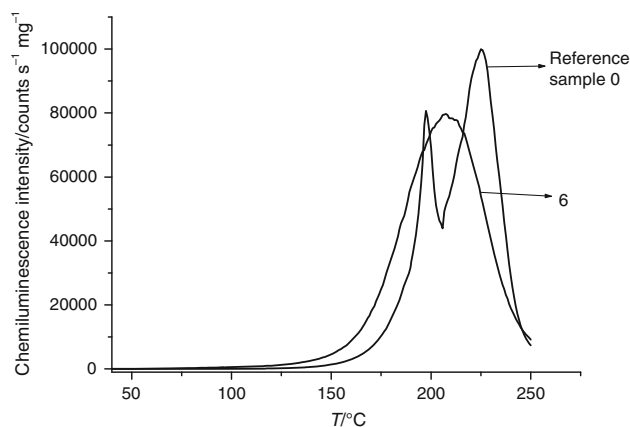


Fig. 10 Nonisothermal chemiluminescence runs in oxygen for nitrocellulose samples 0 and 6, the rate of heating $5\text{ }^{\circ}\text{C min}^{-1}$

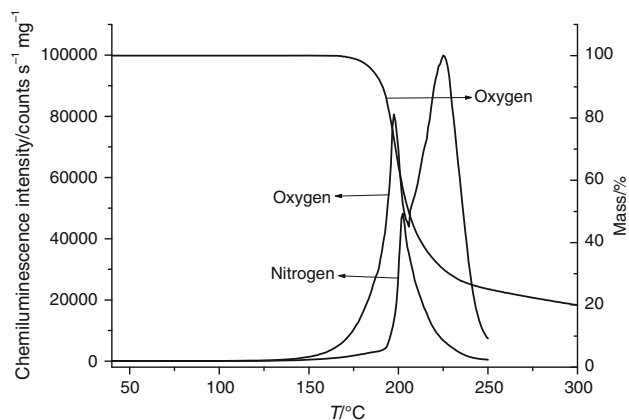


Fig. 11 Non-isothermal chemiluminescence runs in oxygen and nitrogen (the rate of heating $5\text{ }^{\circ}\text{C min}^{-1}$) and thermogravimetry run in oxygen (the rate of heating $10\text{ }^{\circ}\text{C min}^{-1}$) for reference sample 0 of nitrocellulose

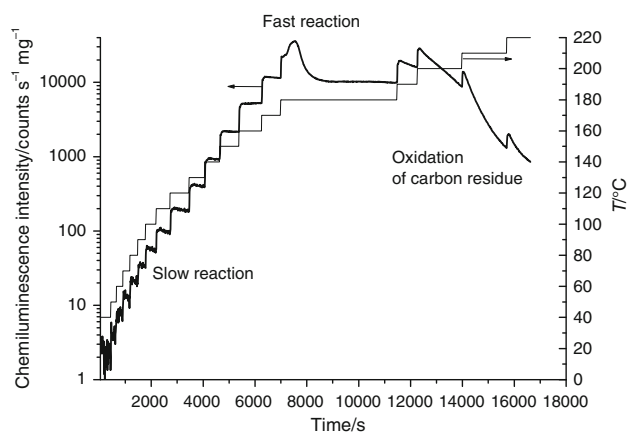


Fig. 12 Stepwisely increased temperature (by $10\text{ }^{\circ}\text{C}$) from 40 to $180\text{ }^{\circ}\text{C}$, and the response of the chemiluminescence emission (in logarithmic coordinate). The temperature was kept constant for some time and measurement occurred under isothermal regime

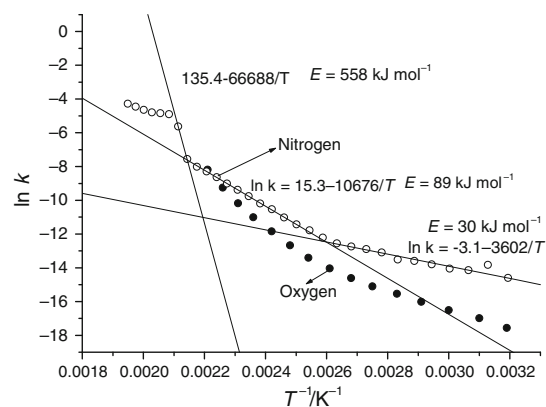
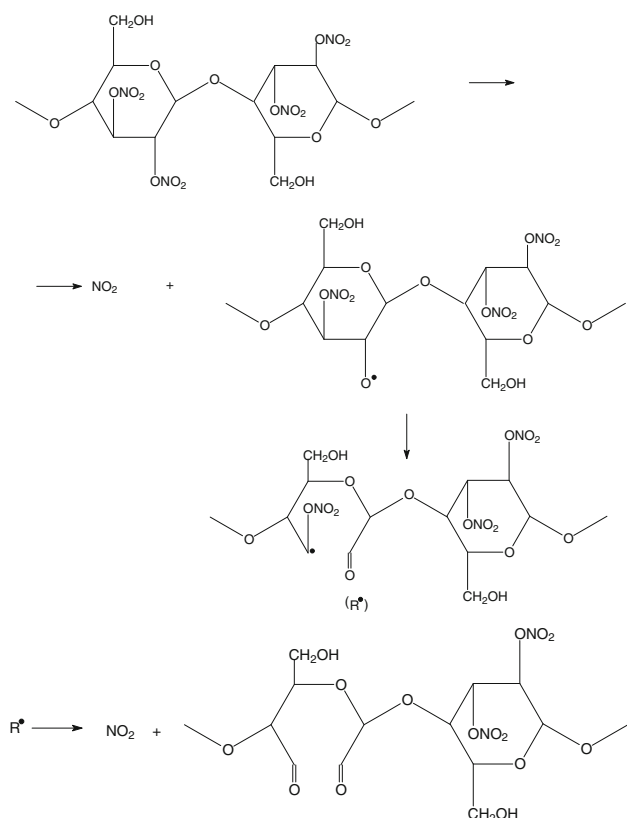


Fig. 13 The Arrhenius' plot for the rate constants from non-isothermal chemiluminescence in nitrogen (reference sample 0—empty points) and from the stationary values of chemiluminescence intensity in oxygen for sample 1—full points, the rate of heating $5\text{ }^{\circ}\text{C min}^{-1}$. The method of evaluation of the rate constants was based on the first order approach described by Eq. 2

remaining service life of the nitrocellulose samples more reliably. One has to have in mind that two slopes are usually observed in the temperature interval of the slow decomposition reaction on the Arrhenius' graph (Fig. 13).

The Table 3 brings an overview of the rate constants of nitrocellulose decomposition determined from TG, DSC and chemiluminescence runs for 50 , 130 , and $200\text{ }^{\circ}\text{C}$, respectively. While relatively good agreement may be seen for $200\text{ }^{\circ}\text{C}$ (the span of the values from 0.003 to 0.02 s^{-1}) with the exception of data from the paper [10] which provides much higher values, the temperature close to ambient ($50\text{ }^{\circ}\text{C}$) gives the span over several orders of magnitude which are typical particularly for non-isothermal TG and DSC measurements. Even data corresponding to temperature $130\text{ }^{\circ}\text{C}$ (the temperature of ageing) are not very far each from the other. It may be of interest that the rate constants from TG increase with the extent of sample ageing. This fact should be considered when treating different nitrocellulose samples of the different storing history.

There are no doubts that the initial step in degradation of nitrocellulose is the splitting of $-\text{O}-\text{NO}_2$ bonds of the secondary nitrate group joined to carbon atoms 2 or 3 of the glucopyranosyl ring (Scheme 1). These bonds have the dissociation energy 167 kJ mole^{-1} , while those at the primary position of carbon atom 6 have dissociation energy about 330 kJ mole^{-1} [13]. The subsequent steps are more the matter of speculation, especially those leading ultimately to a char. One possibility is that in the sequence of β -scissions glucopyranosyl ring may open, the free radicals R^{\bullet} split out another molecule of NO_2 , and finally there appear aldehydes, which are prone to oxidation due to direct reaction with oxygen or in its absence with NO_2 . The transfer reaction to CH_2 bonds on carbon atoms 6 may



Scheme 1 Initial stages of the decomposition of nitrocellulose

induce the splitting off the formaldehyde (Scheme 1). Nitric acid which is formed from NO₂ due to the presence of air humidity will contribute to the cation induced cleavage of glycosidic bonds C–O–C linking glucopyranosyl units and the molar mass of nitrocellulose is reduced. At the same time, after decarbonylation of aldehydic groups the following sequential moieties in the nitrocellulose macromolecules may be formed which form the possible skeleton of the char formed.



Conclusions

Chemiluminescence under nonisothermal conditions appears a very suitable method for the differentiation of auto-accelerating fast decomposition of nitrocellulose starting from 194 °C (the rate of heating 5 °C/min, nitrogen) and the two slow processes at lower temperatures. At the same time, it displays the oxidation of the char being formed in the process. Due to the very stable base line, the rate constants obtained from extrapolation of the slow reaction to lower temperatures appear more reliable than those obtained from thermogravimetry or differential

scanning calorimetry experiments that cover predominantly the temperature region of the fast decomposition reaction.

Acknowledgements The present research has received funding from the European Community's Seventh Framework Programme FP7/2007-2013 under the grant agreement no. 212218—Popart: Strategy for the preservation of plastic artefacts in museum collections. The authors gratefully acknowledge the support from the Grant Agency VEGA, Project No. 2/0115/09. This publication is the result of the project implementation: Centre for materials, layers and systems for applications and chemical processes under extreme conditions, Stage II which was supported by the Research & Development Operational Programme funded by the ERDF.

References

1. Quye A, Littlejohn D, Pethrick RA, Steward RA. Investigation of inherent degradation in cellulose nitrate museum artefacts. *Polym Degrad Stab*. 2011. doi:10.1016/j.polymdegradstab.2011.03.009.
2. Clarkson A, Roberston CM. Refined calculation for determination of nitrogen in nitrocellulose by infrared spectrometry. *Anal Chem*. 1966;38:522.
3. Krabbendam-LaHaye ELM, De Klerk WPC, Krämer RE. The kinetic behavior and thermal stability of commercially available explosives. *J Therm Anal Calorim*. 2005;80:495–501.
4. Makashir PS, Mahajan RR, Agrawal JJ. Studies on kinetics and mechanism of initial thermal decomposition of nitrocellulose. *J Therm Anal Calorim*. 1995;45:501–9.
5. Binke N, Rong L, Zhengquan Y, Yuan W, Rongzu YPH, Qingsen Y. Studies on the kinetics of the first order autocatalytic decomposition reaction of highly nitrated nitrocellulose. *J Therm Anal Calorim*. 1999;58:403–11.
6. Paulik F, Paulik J, Arnold M. TG and TGT investigations of the decomposition of nitrocellulose under quasi-isothermal conditions. *J Therm Anal Calorim*. 1977;12:383.
7. Rong L, Binke N, Yuan W, Zhengquan Y, Rongzu H. Estimation of the critical temperature of thermal explosion for the highly nitrated nitrocellulose using non-isothermal DSC. *J Therm Anal Calorim*. 1999;58:369–73.
8. Phillips RW, Orlick CA, Steinberger R. The kinetics of the thermal decomposition of nitrocellulose. *J Phys Chem*. 1955;59:1034–9.
9. Huwei L, Ruonong F. Studies on thermal decomposition of nitrocellulose by pyrolysis-gas chromatography. *J Anal Pyrolysis*. 1988;14:163–7.
10. Pourmortazavi SM, Hosseini SG, Rahimi Nasrabadi M, Hajimirsadeghi SS, Momenian H. Effect of nitrate content on thermal decomposition of nitrocellulose. *J Hazard Mater*. 2009;162:1141–4.
11. Lin CP, Shu CM. A comparison of thermal decomposition energy and nitrogen content of nitrocellulose in non-fat process of linters by DSC and EA. *J Therm Anal Calorim*. 2009;95:547–52.
12. Meincke A, Hausdorf D, Gadsden N, Baumeister M, Derrick M, Newman R, Rizzo A. Early cellulose nitrate coatings on furniture of the Company of Modern Craftsmen. In: Keneghan B, Egan L (2007) Proceedings of the conference on plastics—looking at the future and learning from the past, Victoria and Albert Museum, London. London: Archetype Publications; 2008. p. 3.
13. Shashoua Y. Conservation of plastics, materials science, degradation and preservation. Oxford: Butterworth Heinemann and Elsevier; 2008. p. 178.

14. Volltrauer HN, Fontijn A. Low-temperature pyrolysis studies by chemiluminescence techniques real time nitrocellulose and PBX decomposition. *Combust Flame*. 1981;41:313–24.
15. Ashby GE. Oxyluminescence from polymers. *J Polym Sci*. 1961; 50:99–106.
16. Barker RE, Daane JH, Rentzepis PM. Thermochemiluminescence of polycarbonate and polypropylene. *J Polym Sci A*. 1965;3: 2033–45.
17. David DJ. Simultaneous photothermal and differential thermal analysis. *Thermochim Acta*. 1972;3:277–89.
18. Schard MP, Russell CA. Oxyluminescence of polymers. I. General behavior of polymers. *J Appl Polym Sci*. 1964;8:985–95.
19. Reich L, Stivala SS. Elements of polymer degradation. New York: McGraw-Hill; 1971. p. 99.
20. Rychlá L, Rychlý J. New concepts in chemiluminescence at the evaluation of thermooxidative stability of polypropylene from isothermal and non-isothermal experiments. In: Jimenez A, Zaikov GE, editors. *Polymer analysis and degradation*. New York: Nova Science Publishers; 2000. p. 124.
21. Rychlý J, Matisová-Rychlá L, Tiemblo P, Gomez-Elvira J. The effect of physical parameters of isotactic polypropylene on its oxidizability measured by chemiluminescence method. Contribution to the spreading phenomenon. *Polym Degrad Stab*. 2001;71:253.
22. Malíková M, Rychlý J, Matisová-Rychlá L, Csomorová K, Janigová I, Wilde HW. Assessing the progress of degradation of polyurethane by chemiluminescence. I. Unstabilised polyurethane. *Polym Degrad Stab*. 2010;95:2367–75.
23. Wynne AM, Wendlandt WW. The thermal light emission properties of alathon. 1. Effect of experimental parameters. *Thermochim Acta*. 1976;14:61–9.
24. Hsueh CH, Wendlandt WW. Effect of some experimental parameters on the oxyluminescence curves of selected materials. *Thermochim Acta*. 1976;99:37–42.
25. Wendlandt WW. The oxyluminescence of polymers. A review. *Thermochemica Acta*. 1984;72:363–72.
26. Hsueh CH, Wendlandt WW. The kinetics of oxyluminescence of selected polymers. *Thermochim Acta*. 1986;99:41–7.
27. Wendlandt WW. The oxyluminescence and kinetics of oxyluminescence of selected polymers. *Thermochim Acta*. 1983;71: 129–37.